Synthesis and Characterization of PET-Based Liquid Crystalline Copolyesters Containing 6-Oxynaphthalene-2-carboxylate and 6-Oxyanthracene-2-carboxylate Units

Michael R. Hibbs,† Marian Vargas,† Jeremy Holtzclaw,† Wendy Rich,† David M. Collard,*,† and David A. Schiraldi‡

School of Chemistry and Biochemistry, Georgia Institute of Technology, Atlanta, Georgia 30332-0400, and Department of Macromolecular Science, Case Western Reserve University, Cleveland, Ohio 44106

Received April 3, 2003; Revised Manuscript Received July 26, 2003

ABSTRACT: Copolymers of poly(ethylene terephthalate) (PET) containing 6-oxy-2-carboxyanthracene (OA) and 6-oxy-2-carboxynaphthalene (ON) structural units are prepared by reactive blending of acetoxyarenecarboxylic acid comonomers with PET. The new copolymers are characterized by ^{1}H and ^{13}C NMR, DSC, dilute solution viscometry, optical microscopy, and wide-angle X-ray diffraction and compared to poly(ethylene terephthalate-*co*-4-oxybenzoate), PET-*co*-OB. Whereas 40 mol % of the OB unit is required to induce liquid crystallinity in PET-*co*-OB, only 20 mol % of OA or 30 mol % of ON units are required. This is also in contrast to copolymers containing similar amounts of symmetrical arenedicarboxylate structural units which do not form liquid crystalline phases.

Introduction

Since their discovery in the 1970s, liquid crystalline (LC) polymers have been heralded as the second generation of engineering plastics.[1−4] Thermotropic main chain liquid crystalline polymers (LCPs) have rigid backbones which can be aligned by shear strain and elongational flow during processing. The resulting highly ordered materials have excellent mechanical, chemical, and thermal properties. Despite their remarkable properties, sales of commercial LCPs remain low (10 million lb/year in the U.S.),[5] primarily because the selling prices of LCPs are often 10−20 times greater than those of traditional thermoplastics such as poly(ethylene terephthalate) (PET).[6]

Poly(ethylene naphthalate) (PEN) has become competitive with PET in certain performance-driven applications because it has superior strength, heat stability, and gas barrier properties.[7,8] In addition to the longer rigid arylene unit of PEN (2,6-naphthalene, relative to the 1,4-phenylene unit of PET), rotation of the naphthalene unit requires a crankshaft mechanism which necessitates a large displacement of the polymer chain. It is this combination of larger aryl units and restricted rotation that leads to the superior physical properties of PEN relative to PET.[9] However, despite the rigidity of its backbone, PEN does not form an ordered mesophase. PEN remains an expensive alternative to PET, and preparation of PET/PEN blends and PET-*co*-N copolymers in general have properties that are intermediate between those of the two homopolymers.[10−12]

Many attempts have been made to incorporate comonomers into PET to form materials with enhanced properties and which display liquid crystallinity. Jackson and Kuhfuss first described the preparation and liquid crystallinity of PET-*co*-oxybenzoate (abbreviated here as PET-*co*-OB), currently sold commercially as Rodrun LC-5000.[13−15] PET-*co*-OB is prepared by reactive blending of PET and *p*-acetoxybenzoic acid (ABA) to facilitate transesterification with loss of acetic acid to incorporate oxybenzoate units into the polymer. PET-*co*-OB is an LCP when the fraction of oxybenzoate repeat units is at least 40 mol %. The tensile strength and flexural modulus of PET-*co*-OB are maximized at compositions with 60−70 mol % oxybenzoate.[13,16] Oxybenzoate units are components of many other LC copolyesters.[17−19] Important features of the oxybenzoate unit appear to be the collinearity of the substituents and its permanent dipole moment. The largely random sequence of structural units in the copolymers decreases crystallinity while still allowing for high alignment of the polymer chains. The high cost of ABA relative to terephthalic acid, together with the high proportion of ABA required to produce PET-based LCPs, makes the cost of PET-*co*-OB high enough to limit its applications. Thus, it is desirable to design PET-based copolymers that require less than 40 mol % of a comonomer to render them liquid crystalline.

Incorporation of the analogous naphthalene derivative, 6-acetoxy-2-naphthoic acid (ANA), into copolyesters also leads to materials with enhanced properties. For example, whereas poly(oxybenzoate) itself is not liquid crystalline, copolymerization of ABA and ANA affords materials that form nematic mesophases over a broad range of compositions. Vectra is a commercially available LCP typically containing a 73:27 ratio of oxybenzoate and oxynaphthoate units. Similar to the 2,6-naphthalenedicarboxylate unit in PEN, the substituents at the 2- and 6-positions of the oxynaphthoate unit are not collinear. This offset disrupts chain packing without sacrificing chain stiffness. Thus, the melting temperature of Vectra is about 290 °C compared to the oxybenzoate homopolymer, which does not melt below 450 °C.[20]

Efforts to modify PET with rigid comonomers such as dimethyl 2,6-anthracenedicarboxylate[21] and dimethyl 4,4′-bibenzoate (BB)[22] have not yielded LCPs. These monomers are rigid rods, but they do not have permanent dipole moments, a characteristic common to many

† Georgia Institute of Technology.
‡ Case Western Reserve University.
* Corresponding author: e-mail david.collard@chemistry.gatech.edu.

10.1021/ma034425s CCC: $25.00
Published on Web 09/06/2003

mesogenic structural units in main chain LCPs. However, fibers drawn from PET-*co*-BB show much greater orientation (and consequently greater tensile strength) than PET but do not show the birefringence of an LCP. The compositions of PET-*co*-BB that show high orientability are those with a high percentage (>40 mol %) of comonomer and have been described as frustrated liquid crystalline polymers.[23]

Despite the widespread use of ANA to prepare LCPs, and its structural similarity to ABA, preparation of the copolymer PET-*co*-oxynaphthoate (PET-*co*-ON) has not been reported. The three-ring analogue of ANA, 6-acetoxy-2-anthracenoic acid (AAA), also has noncollinear substituents at the 2- and 6-positions. AAA has a greater aspect ratio than ANA or ABA, but its synthesis has not been reported. Given the widespread use of PET in a variety of applications, and formation of LC phases with >40 mol % ABA, we set out to investigate the possibility that PET-*co*-ON and the copolyester derived from AAA would form LC phases with smaller amounts of comonomer.

Here we describe the synthesis of AAA and the preparation of the copolymers PET-*co*-ON and PET-*co*-oxyanthracenoate (PET-*co*-OA). The compositions of the copolymers are varied in order to determine the mol % of each oxyarenecarboxylate that is required to form an LCP. For convenience, the copolyesters are designated as PETX-*y*, where X denotes the comonomer unit (OB = 4-oxybenzoate, ON = 6-oxy-2-naphthoate, and OA = 6-oxy-2-anthracenoate) and *y* indicates the mol % of the oxyarenecarboxylate structural unit.

Experimental Section

Materials. Chloroform was washed with water and dried over $MgSO_4$ prior to distillation from P_2O_5. Dichloromethane was stored over 4 Å molecular sieves prior to distillation from calcium hydride. All other materials were used as received from Aldrich Chemical Co., except PET which was obtained from KoSa (Spartanburg, SC). 6-Acetoxy-2-naphthoic acid (ANA) was prepared from 6-hydroxy-2-naphthoic acid by a previously reported method.[24]

Characterization. ^{1}H and ^{13}C nuclear magnetic resonance (NMR) spectra were obtained on a Bruker AMX 400 MHz instrument operating at 400.1 and 100.6 MHz, respectively. Polymer samples were dissolved in a ca. 9:1 (v/v) mixture of $CDCl_3$ and deuterated trifluoroacetic acid (TFA-*d*), and chemical shifts were measured with respect to internal tetramethylsilane (TMS). For the ^{13}C NMR spectra, a spectral width of 33 kHz, relaxation delay of 3 s, and inverse gated decoupling were used to eliminate the nuclear Overhauser effect (nOe) and optimize collection of spectra.

Infrared characterization was performed using a Nicolet 520 FTIR spectrophotometer. Melting points were collected using a Laboratory Devices Mel-Temp II melting point apparatus. High-resolution mass spectra were obtained on a VG Instruments 70-SE mass spectrometer using electron impact ionization.

Dilute solution viscometry was performed on an AVS 500 viscometer at 25 °C using a 1% polymer solution in dichloroacetic acid. Molecular weights, M_v, for PET copolymers were approximated by using the Mark−Houwink coefficients for PET ($K = 1.7 \times 10^{-4}$, $a = 0.83$).

Differential scanning calorimetry (DSC) was performed using a Perkin-Elmer series 7 differential scanning calorimeter. The temperature program provided heating and cooling cycles between 50 and 275 °C at 10 °C/min. Polymers were studied for birefringence using a Leica DMRX polarizing microscope equipped with a heating stage. Microscopy samples were prepared by compressing molten polymer samples between two untreated glass slides. X-ray diffraction patterns were obtained with a SCINTAG X1 diffractometer with Cu Kα radiation (45 kV, 40 mA) and a Peltier-cooled solid-state detector.

2,5-Dimethyl-4′-methoxybenzophenone, 1. *p*-Anisoyl chloride (100.48 g, 588.98 mmol) was added dropwise over 2 h to a stirred mixture of $AlCl_3$ (94.24 g, 706.8 mmol) in *p*-xylene (202 mL, 1.64 mol) at 10−20 °C under N_2. The reaction mixture was stirred for an additional 20 min, and 300 mL of CH_2Cl_2 was added. H_2O (200 mL) was added over 30 min. The mixture was filtered, the layers were separated, and the solvent was removed from the organic portion by distillation under reduced pressure. The residue was dissolved in 400 mL of CH_2Cl_2 and was washed with 10% NaOH (100 mL) and water (100 mL). The solution was dried over $MgSO_4$, and the solvent was removed under reduced pressure to yield **1** as an off-white solid (118.09 g, 83%); mp 89−90 °C (lit.[25] mp 88−89 °C). ^{1}H NMR (300 MHz, $CDCl_3$): δ 7.79 (d, $J_{ortho} = 9$ Hz, 2H), 7.16 (m, 2H), 7.09 (s, 1H), 6.93 (d, $J_{ortho} = 9$ Hz, 2H), 3.88 (s, 3H, $-OCH_3$), 2.33 (s, 3H), 2.24 (s, 3H). IR (KBr): 1651 (C=O str), 1256 (C−O−C asym str), 1020 cm^{-1} (C−O−C sym str). HRMS (EI) calcd for $C_{16}H_{16}O_2$: 240.11503. Found: 240.11324.

(4-Methoxybenzoyl)terephthalic Acid, 6. A solution of 2,5-dimethyl-4′-methoxybenzophenone (**1**) (50.01 g, 208.1 mmol), pyridine (525 mL), and H_2O (700 mL) was stirred and heated to reflux. $KMnO_4$ (197.3 g, 1.248 mol) was added portionwise over 75 min, and the mixture was heated at reflux for an additional 5 h. The mixture was cooled, and the precipitated MnO_2 was removed by filtration. The filtrate was heated at reflux, and more $KMnO_4$ (197.3 g, 1.248 mol) was added portionwise over 75 min. The mixture was heated at reflux for an additional 5 h and cooled to room temperature, and the mixture was filtered. This two-step addition of $KMnO_4$ was used to avoid lack of mass transfer in the heterogeneous mixture which resulted if the $KMnO_4$ was added in a single step. The filtrate was cooled in an ice−water bath, and H_2SO_4 (20%) was added carefully until the pH was below 7. The resulting precipitate was collected by filtration and redissolved in a 10% Na_2CO_3 solution (300 mL). The solution was cooled in an ice−water bath and was reacidified with H_2SO_4 (20%). The resulting precipitate was collected by filtration and dried under reduced pressure to yield **6** as a white solid (49.11 g, 79%); mp 278−282 °C. ^{1}H NMR (300 MHz, DMSO-d_6): δ 8.15 (dd, $J_{ortho} = 9$ Hz, $J_{meta} = 2$ Hz, 1H), 8.06 (d, $J_{ortho} = 9$ Hz, 1H), 7.80 (d, $J_{meta} = 2$ Hz, 1H), 7.61 (d, $J_{ortho} = 9$ Hz, 2H), 7.02 (d, $J_{ortho} = 9$ Hz, 2H), 3.81 (s, 3H, $-OCH_3$). IR (KBr): 3440−2550 (O−H str), 1703 (C=O str, COOH), 1664 (C=O str, ketone), 1427 (C−O−H bend), 1315 (C−O str), 1262 cm^{-1} (C−O−C asym str). HRMS (EI) calcd for $C_{16}H_{12}O_6$: 300.06339. Found: 300.06311.

[(4-Methoxyphenyl)methyl]terephthalic Acid, 8. A mixture of (4-methoxybenzoyl)terephthalic acid (**6**) (34.20 g, 113.9 mmol), triethylsilane (54.5 mL, 341 mmol), trifluoroacetic acid (115 mL), and chloroform (115 mL) was stirred and heated at reflux for 48 h. A second portion of triethylsilane (18.2 mL, 114 mmol) was added, and the mixture was heated at reflux for an additional 72 h. The reaction mixture was cooled and slowly poured into Na_2CO_3 (68 g, 642 mmol) dissolved in 272 mL of water. Concentrated HCl was added to the aqueous layer until the pH was less than 7. The precipitate was collected by filtration and dissolved in 75 mL of 10% aqueous NaOH solution. The solution was washed with 50 mL of Et_2O, and HCl was added to the aqueous layer until the pH was less than 7. The precipitate was collected by filtration, triturated with 200 mL of cold water, and dried under reduced pressure to yield **8** as a white solid (28.37 g, 87%); mp 275−276 °C (lit.[26] 265−266 °C). ^{1}H NMR (300 MHz, DMSO-d_6): δ 7.85−7.77 (m, 3H), 7.07 (d, $J_{ortho} = 7$ Hz, 2H), 6.82 (d, $J_{ortho} = 7$ Hz, 2H), 4.27 (s, 2H, CH_2), 3.69 (s, 3H, $-OCH_3$). IR (KBr): 3350−2540 (O−H str), 1703 (C=O str), 1410 (C−O−H bend), 1302 (C−O str), 1256 (C−O−C asym str) cm^{-1}. HRMS (EI) calcd for $C_{16}H_{14}O_5$: 286.08412. Found: 286.08845.

3-Carboxy-7-methoxy-9(10*H*)-anthracenone, 9. A mixture of [(4-methoxyphenyl)methyl]terephthalic acid (**8**) (13.78 g, 48.13 mmol), oxalyl chloride (26.0 mL, 298 mmol), DMF (6 drops), and CH_2Cl_2 (60 mL) was stirred and heated at reflux

for 18 h. Excess oxalyl chloride and CH_2Cl_2 were removed by distillation under reduced pressure. CS_2 (200 mL) was added to the residue, and the resulting mixture was added to a stirred mixture of $AlCl_3$ (14.74 g, 110.5 mmol) and CS_2 (200 mL) at 0 °C over 75 min under N_2. When the addition was complete, the stirred mixture was allowed to warm to room temperature over 4 h. Water (140 mL) was carefully added to quench the reaction. After mixing thoroughly, the reaction mixture was filtered and the solid was combined with the CS_2 layer of the filtrate. The solvent was removed by distillation, and the residue was dried under reduced pressure to yield **9** as a yellow solid which was used without further purification (9.421 g, 73%); mp 325 °C (dec). In DMSO solution, **9** is in equilibrium with its tautomer, 10-hydroxy-6-methoxy-2-anthracenoic acid, **9a**. 3-Carboxy-7-methoxy-9(10*H*)-anthracenone, **9**: ^{1}H NMR (300 MHz, DMSO-d_6): δ 8.26 (d, J_{ortho} = 8 Hz, 1H, Ar−H_4), 8.13 (s, 1H, Ar−H_1), 7.99 (d, J_{ortho} = 8 Hz, 1H, Ar−H_3), 7.62 (d, J_{meta} = 3 Hz, 1H, Ar−H_5), 7.53 (d, J_{ortho} = 8 Hz, 1H, Ar−H_8), 7.31 (dd, J_{ortho} = 8 Hz, J_{meta} = 3 Hz, 1H, Ar−H_7), 4.43 (s, 2H, CH_2), 3.94 (s, 3H, −OCH_3). 10-Hydroxy-6-methoxy-2-anthracenoic acid, **9a**: ^{1}H NMR (300 MHz, DMSO-d_6): δ 8.62 (s, 1H, Ar−H_9), 8.41 (d, J_{ortho} = 9 Hz, 1H, Ar−H_4), 8.19 (s, 1H, Ar−H_1), 7.94 (d, J_{ortho} = 9 Hz, 1H, Ar−H_8), 7.80 (d, J_{ortho} = 9 Hz, 1H, Ar−H_3), 7.73 (d, J_{meta} = 2 Hz, 1H, Ar−H_5), 7.19 (dd, J_{ortho} = 9 Hz, J_{meta} = 2 Hz, 1H, Ar−H_7), 3.93 (s, 3H, −OCH_3). IR (KBr): 3450−2850 (O−H str), 1705 (C═O str, COOH), 1657 (C═O str, ketone), 1405 (C−O−H bend), 1302 (C−O str), 1223 cm^{-1} (C−O−C asym str). HRMS (EI) calcd for $C_{16}H_{12}O_4$: 268.07356. Found: 268.07231.

6-Methoxy-2-anthracenoic Acid, 5. A mixture of 3-carboxy-7-methoxy-9(10*H*)-anthracenone (**9**) (10.00 g, 37.28 mmol) and zinc dust (14.79 g, 226.3 mmol) in 200 mL of 5% aqueous NaOH was stirred and heated at reflux for 4 h. The mixture was cooled and filtered. The solid was placed in a Soxhlet extraction thimble, and the filtrate was used to extract product from the solid for 48 h. 10% HCl was added to the cooled extract until the pH was below 7. The precipitate was collected by filtration and dried under reduced pressure to yield **5** as a yellow solid (6.629 g, 70%); mp 305−307 °C (lit.[27] 288−289 °C). ^{1}H NMR (300 MHz, DMSO-d_6): δ 8.72 (s, 1H, Ar−H_9), 8.70 (s, 1H. Ar−H_1), 8.44 (s, 1H, Ar−H_{10}), 8.05 (d, J_{ortho} = 8 Hz, 1H, Ar−H_4), 8.02 (d, J_{ortho} = 9 Hz, 1H, Ar−H_8), 7.88 (dd, J_{ortho} = 8 Hz, J_{meta} = 2 Hz, 1H, Ar−H_3), 7.41 (d, J_{meta} = 2 Hz, 1H, Ar−H_5), 7.22 (dd, J_{ortho} = 9 Hz, J_{meta} = 2 Hz, 1H, Ar−H_7), 3.92 (s, 3H, −OCH_3). IR (KBr): 3300−2850 (O−H str), 1703 (C═O str), 1420 (C−O−H bend), 1295 (C−O str), 1223 cm^{-1} (C−O−C asym str). HRMS (EI) calcd for $C_{16}H_{12}O_3$: 252.07864. Found: 252.07873.

6-Hydroxy-2-anthracenoic Acid, 10. A mixture of 6-methoxy-2-anthracenoic acid (**5**) (3.12 g, 12.4 mmol) and 48% HBr (11.0 mL, 97.2 mmol) in 60 mL of acetic acid was stirred and heated at reflux for 3 h. The mixture was poured into 250 mL of cold water. The precipitate was collected by filtration and dried under reduced pressure to yield **10** as a green solid which was used without further purification (1.77 g, 60%); mp 275−278 °C. ^{1}H NMR (300 MHz, DMSO-d_6): δ 8.68 (s, 1H, Ar−H_9), 8.64 (s, 1H, Ar−H_1), 8.30 (s, 1H, Ar−H_{10}), 8.00 (d, J_{ortho} = 9 Hz, 1H, Ar−H_4), 8.00 (d, J_{ortho} = 9 Hz, 1H, Ar−H_8), 7.83 (d, J_{ortho} = 9 Hz, 1H, Ar−H_3), 7.24 (d, J_{meta} = 2 Hz, 1H, Ar−H_5), 7.18 (dd, J_{ortho} = 9 Hz, J_{meta} = 2 Hz, 1H, Ar−H_7). IR (KBr): 3500−2900 (O−H str), 1703 (C═O str), 1427 cm^{-1} (C−O−H bend). HRMS (EI) calcd for $C_{15}H_{10}O_3$: 238.06299. Found: 238.06209.

6-Acetoxy-2-anthracenoic Acid, 11. A mixture of 6-hydroxy-2-anthracenoic acid (**10**) (9.663 g, 40.56 mmol), pyridine (29.5 mL, 365 mmol), and acetic anhydride (123.0 mL, 1.221 mol) was stirred at room temperature for 19 h. The mixture was poured into 600 mL of cold water, and the precipitate was triturated with 270 mL of 1% HCl. The solid was added to 150 mL of acetone and 50 mL of water, and the mixture was heated at reflux for 22 h. After cooling, the solid was collected by filtration and recrystallized from an acetone/water mixture (380 mL/38 mL) to yield **11** as a yellow solid (5.62 g, 49%); mp 289−291 °C. ^{1}H NMR (300 MHz, DMSO-d_6): δ 8.84 (s, 1H, Ar−H_9), 8.79 (s, 1H, Ar−H_1), 8.61 (s, 1H, Ar−H_{10}), 8.17 (d, J_{ortho} = 9 Hz, 1H, Ar−H_8), 8.13 (d, J_{ortho} = 9 Hz, 1H, Ar−H_4), 7.93 (dd, J_{ortho} = 9 Hz, J_{meta} = 2 Hz, 1H, Ar−H_3), 7.84 (d, J_{meta} = 2 Hz, 1H, Ar−H_5), 7.37 (dd, J_{ortho} = 9 Hz, J_{meta} = 2 Hz, 1H, Ar−H_7), 2.34 (s, 3H, CH_3). IR (KBr): 3200−2500 (O−H str), 2644−2552 (aliph C−H str), 1769 (C═O str, ester), 1690 (C═O str, COOH), 1433 (C−O−H bend), 1210 cm^{-1} (acetate C(═O)−O str). HRMS (EI) calcd for $C_{17}H_{12}O_4$: 280.07356. Found: 280.07357.

Preparation of Copolymers. The preparation of a PET-*co*-OA10 is described here to illustrate the preparation of copolymers. PET pellets (4.520 g, 90 mol %) and **11** (0.739 g, 10 mol %) were placed in a glass reaction vessel equipped with a mechanical stirrer, nitrogen inlet, distillation head, and condenser. The reaction vessel was purged with N_2, and the mixture was heated under N_2 for 30 min at 300 °C, during which time it formed a homogeneous melt. The N_2 flow was stopped, and the pressure was gradually reduced over 10 min to <1 mmHg. The reaction temperature was lowered to 275 °C over 30 min and was held there for 3.5 h, during which water was removed by distillation. The total reaction time was 4.5 h, with the reaction temperature above 275 °C for only the first hour. Upon cooling, the polymer was removed from the reactor by dissolving it in a ca. 1:1 (v/v) mixture of $CHCl_3$ and trifluoroacetic acid (TFA). The polymer was reprecipitated by pouring the solution into an excess of MeOH. The solid was washed thoroughly with MeOH and dried in a vacuum oven.

Incorporation of 4-acetoxybenzoic acid and 6-acetoxy-2-naphthoic acid into PET was performed in a similar fashion, except that the reaction temperature was held at 275 °C throughout the procedure. PET-*co*-OA30 and PET-*co*-OA40 did not completely dissolve, but they were removed from the reactor by forming slurries with $CHCl_3$ and TFA which were poured into MeOH.

Samples of the polymers were subjected to solid-state polymerization (SSP) by placing the polymer in a flask at reduced pressure (<0.2 mmHg). The flask was placed in a heated oil bath (180−210 °C) for ca. 24 h. The temperature of the SSP was chosen to be about 10 °C below the onset of melting of the polymer.

Results and Discussion

Monomer Synthesis. A 10-step synthesis of 6-methoxy-2-anthracenoic acid, **5**, from *p*-anisic acid has been previously reported with a 13% overall yield.[26,28] That synthetic scheme involved preparation of 2-methoxy-6-methylanthracene and the subsequent oxidation of the methyl substituent to form the carboxylic acid. However, this approach required steps to protect the 9- and 10-positions of the anthracene core from oxidation, which would give the corresponding anthraquinone. To avoid the protection and deprotection steps, shorten the synthesis, and improve the overall yield, we focused on synthetic schemes in which the oxidation step takes place prior to formation of the anthracene ring system.

Our synthesis of 6-acetoxy-2-anthracenoic acid (**11**) as a monomer for incorporation into copolyesters is outlined in Schemes 1 and 2. The original strategy was to prepare **11** by a synthetic route similar to that used to make dimethyl 2,6-anthracenedicarboxylate in which the fused ring system was prepared by a thermally promoted Elbs reaction[29] of an appropriately substituted 2-methylbenzophenone.[21] The first step was a Friedel−Crafts acylation of *p*-xylene with *p*-anisoyl chloride to yield 2,5-dimethyl-4′-methoxybenzophenone, **1**. However, attempts to ring-close **1** by the Elbs reaction gave anthrone **2** and anthraquinone **3** (Scheme 1) in only 35% yield. Oxidation of mixtures of **2** and **3** with CrO_3 afforded very low yields (17%) of the anthraquinone acid, **4**, which could then be reduced to the corresponding anthracene, **5**. Although this reaction sequence

Scheme 1. Synthesis of Precursors to Anthracene Monomer, 11[a]

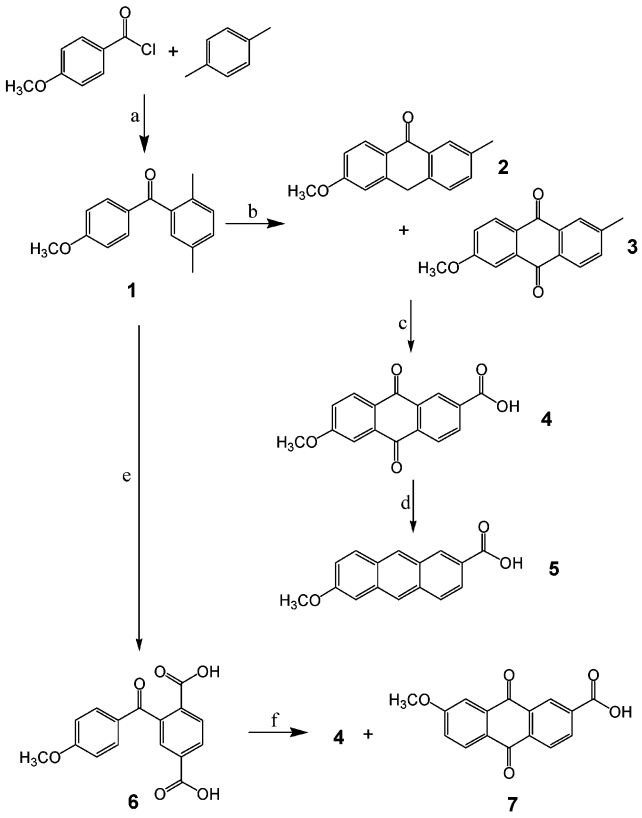

[a] (a) $AlCl_3$, 10−20 °C, 2 h; (b) air, 310−340 °C, 24 h; (c) CrO_3, H_2SO_4, AcOH, Ac_2O, Δ, 18 h; (d) Zn, NH_4OH, H_2O, Δ, 8 h; (e) $KMnO_4$, pyridine, H_2O, Δ, 10 h; (f) polyphosphoric acid, 150 °C, 3 h.

Scheme 2. Synthesis of Anthracene Monomer, 11[a]

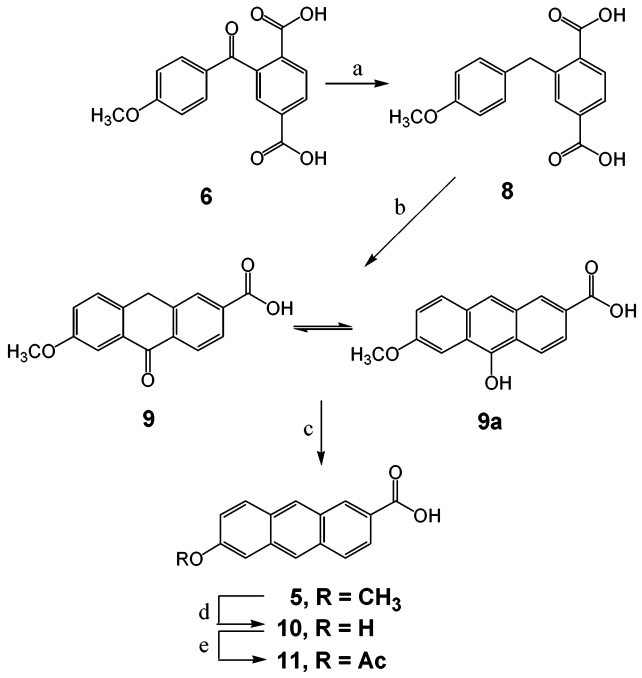

[a] (a) Et_3SiH, CF_3COOH, $CHCl_3$, Δ, 120 h; (b) i. $(COCl)_2$, CH_2Cl_2, DMF, Δ, 18 h; ii. $AlCl_3$, CS_2, 0 °C, 5 h; iii. H_2O; (c) Zn, NaOH, H_2O,Δ, 3.5 h; (d) HBr, AcOH, Δ, 3 h; (e) Ac_2O, pyridine, 25 °C, 19 h.

yielded **5** in only four steps, the yields from both the ring-closing and oxidation steps were unacceptably low.

Scheme 3. Hayashi Rearrangement of (4-Methoxybenzoyl)terephthalic Acid[a]

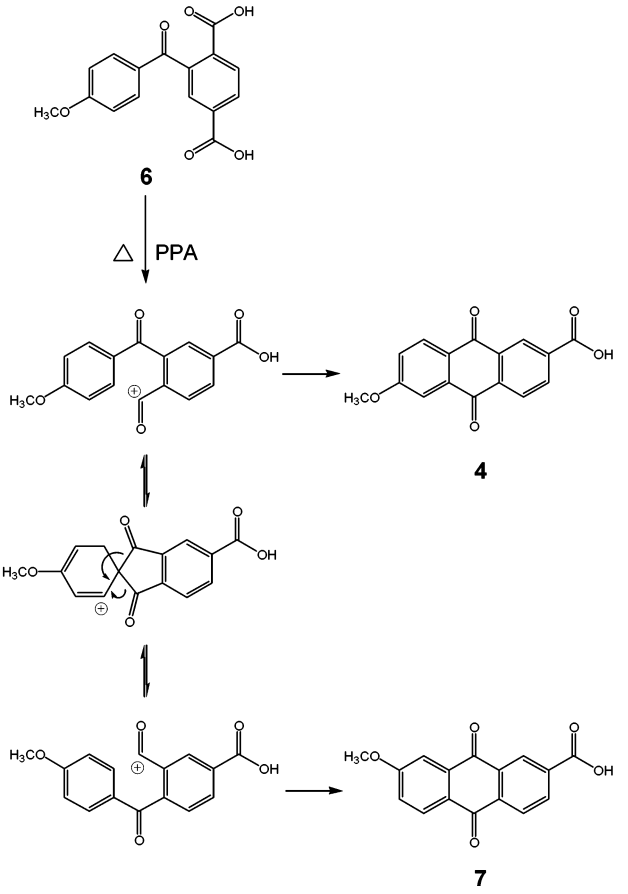

[a] See ref 33 for other examples of the Hayashi rearrangement.

We turned our attention to the possibility of forming the anthracene ring system via ring closure of a 2-carboxybenzophenone by a Friedel−Crafts reaction. Oxidation of **1** was accomplished by modifying a procedure reported for the oxidation of substituted 2-methylbenzophenones[30] to afford diacid **6** (Scheme 1). Attempts to perform an intramolecular Friedel−Crafts acylation of **6** in H_2SO_4[31] did not yield any ring-closed product. Use of polyphosphoric acid[32] gave low yields of regioisomeric anthraquinones **4** and **7**. (The ^1H NMR spectrum of the mixture included two well-resolved doublets of equal intensity for H-8 of **4** and H-5 of **7**.) This mixture of isomers arises from a Hayashi rearrangement[33] in which a key spirocation intermediate can open in two ways to give the two regioisomeric products (Scheme 3). The spirocation forms when electrophilic attack by the initially formed acylium cation takes place at the ipso carbon on the adjacent aryl ring of the benzophenone (i.e., C-1′) to form a five-membered ring rather than at the ortho carbon (C-2′) which is deactivated by the carbonyl substituent.

To increase the electron density of the ortho carbon and thereby avoid formation of the spirocation, it was necessary to reduce the ketone of **6** to afford the diphenylmethane derivative **8** (Scheme 2). Attempts to reduce **6** by either Wolff−Kishner[34] or Clemmensen[35] reactions gave complex mixtures of products. Conversion of **6** to **8** was accomplished by hydrogenation over palladium on carbon in methanol.[36] Reduction with triethylsilane in trifluoroacetic acid[37] proved to be more practical for large-scale (multigram) reactions.Conver-

Scheme 4. Proposed Pathways for Substitution Reactions of the C-2 Substituent during Attempts To Reduce Anthrone 9[a]

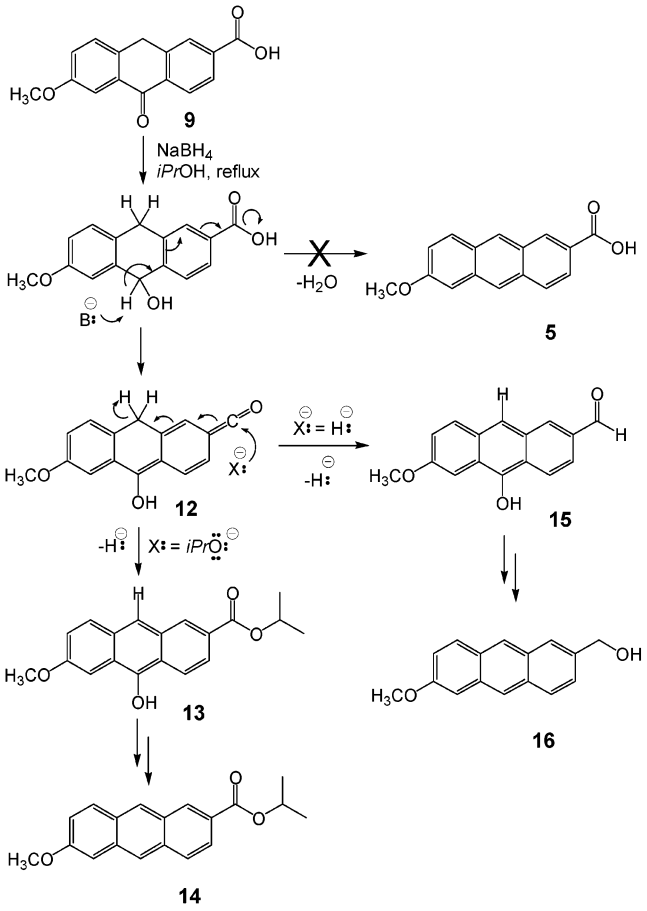

[a] See ref 40 for example of a *p*-quinoid ketene.

sion of the benzophenone to the diphenylmethane derivative removes the electron-withdrawing ketone which deactivated the ortho position. While the 1-position of **8** is still activated by the 4-methoxy substituent, the 2-position is now activated by the benzyl substituent on C-1′ and ring-closure to form the six-membered ring at C-2′ becomes competitive with closure of the five-membered ring (at C-1′).

Diacid **8** was converted to the corresponding di(acid chloride) which was subjected to Friedel−Crafts acylation to form the anthrone ring. The unreacted acid chloride in the 2-position was hydrolyzed to the carboxylic acid during workup to yield **9** containing aluminum oxide as an impurity. In polar solvents such as DMSO, the equilibrium constant for the tautomerization of **9** to **9a** is great enough that the ^{1}H NMR spectrum of **9** in DMSO-d_6 has peaks corresponding to both tautomers (Scheme 2).[38] In $CDCl_3$ only peaks for **9** were observed in the ^{1}H NMR spectrum.

Initial attempts to reduce anthrone **9** using $NaBH_4$ in isopropyl alcohol[39] gave mixtures of isopropyl 6-methoxy-2-anthracenoate, **14**, and 2-hydroxymethyl-6-methoxyanthracene, **16**. A proposed pathway for these reactions is shown in Scheme 4 whereby the doubly benzylic carbon of the initially formed dihydroanthrol intermediate undergoes deprotonation to give the *p*-quinoid ketene,[40] **12**. This reaction to form the conjugated ketene proceeds faster than dehydration of the central ring to form the anthracene core of **5**. Addition of isopropoxide or hydride to ketene **12** gives the ester **13** and the aldehyde **15**, respectively. Further reduction of **13** and **15** in the presence of $NaBH_4$ gives the observed products **14** and **16**.

Anthrone **9** was successfully reduced to anthracene **5** by reaction with zinc in aqueous NaOH[41] (Scheme 2). The sodium salt of **5** is partially soluble in water, so the reaction mixture was filtered and extracted with water in a Soxhlet extractor to separate the salt of **5** from the zinc and the aforementioned aluminum oxide. Addition of HCl to the aqueous extract led to the precipitation of **5**. It was important to stop the zinc reduction after 3−4 h in order to avoid overreduction leading to the formation of 9,10-dihydro-6-methoxy-2-anthracenoic acid. This overreduced byproduct could be oxidized back to anthracene analogue **5** by treatment with DDQ in benzene,[21] but its formation could be avoided by limiting the time of the reduction reaction. Thus, our synthesis affords **5** in six steps with a 29% yield from *p*-anisoyl chloride and is a significant improvement on the previous synthesis.

Methyl ether **5** was converted to alcohol **10** by treatment with aqueous HBr in refluxing acetic acid.[42] Reaction of **10** and acetic anhydride[23] gives the desired monomer, **11**.

Preparation of Copolymers. In the reactive blending of acetoxyarene carboxylic acids with PET, the initial acidolysis step results in a reaction mixture with a relatively low melt viscosity. PET chains are cleaved during acidolysis by free carboxylic acids, the majority of which come from the acetoxyarene carboxylic acid monomer, although the PET starting material also has some acid end groups. Acidolysis is followed by condensation of carboxylic acid and acetoxy end groups (which may be located on either monomers or oligomers) with removal of acetic acid and an increase in melt viscosity and molecular weight. This condensation reaction proceeds through the transfer of an acyl group from the phenolic oxygen atom to an acid to form a mixed anhydride which is subsequently attacked by the phenol (or an alcohol end group in the PET starting material) to yield an ester and acetic acid which is removed from the polymerization mixture.[43]

Transesterification of acetoxyarenecarboxylic acids ABA, ANA, and AAA with PET at 270 °C under vacuum resulted in the removal of acetic acid and the formation of a cloudy polymer melt. The samples were cooled, dissolved in TFA, and reprecipitated into methanol before they were heated under vacuum at temperatures slightly below the onset of melting in order to increase molecular weights by solid-state polymerization. The viscosity average molecular weights, M_v, of the copolymers were calculated using Mark−Houwink constants for PET (Table 1). As in the case of poly(ethylene terephthalate-*co*-2,6-anthracene dicarboxylate) with moderate levels (>20 mol %) of the symmetrically substituted anthracene-containing structural unit with no net dipole moment, PET-*co*-OA40 is not soluble in dichloroacetic acid. The range of viscosity average molecular weights is considerable but understandable given the differences in the rigidity of the various copolymer backbones and our use of Mark−Houwink constants for the PET homopolymer.

Structural Characterization. ^{1}H NMR spectroscopy was performed on wholly soluble polymers. (Partially soluble copolymers were not studied in detail to avoid differences arising from fractionation.) The relative amount of oxyarenecarboxylate units that was

Table 1. Composition of Copolymers

	% comonomer incorporated[a]	M_v (g/mol)[b]	EA end groups ($\times 10^{-5}$ mol/g)[a,c]
PET	0	19 300	0
PET-*co*-OB40	36	20 900	5.7
PET-*co*-ON20	18	12 300	8.1
PET-*co*-ON30	30	13 300	13
PET-*co*-ON40	39	28 000	3.6
PET-*co*-OA10	9	12 300	11
PET-*co*-OA15	16	12 000	15
PET-*co*-OA20	20	10 700	16
PET-*co*-OA30	26	16 500	12
PET-*co*-OA40	[d]	[d]	[d]

[a] Determined by ^{1}H NMR. [b] Intrinsic viscosity measured in dichloroacetic acid solution; M_v calculated using Mark−Houwink constants for PET. [c] EA = ethylene acetate; the PET starting material had 7.9×10^{-5} mol/g ethylene glycol (EG) end groups. [d] Not determined owing to insolubility of copolymer.

incorporated into the copolymers was determined by comparing the sum of the integrals of all the aryl peaks with the integral of the peak arising from the ethylene glycol units. The results show that the polymerizations were successful in preparing copolymers with the desired ratios of PET and oxyarenecarboxylate units (Table 1).

The ^{1}H NMR spectra indicate that the copolymers have ethylene acetate (EA) end groups (Table 1). The concentration of EA end groups is consistent with the number of ethylene glycol (EG) end groups in the PET starting material (as determined by using an acid/base titration to measure the number of acid end groups and then assuming that all other end groups were EG end groups, Table 1 footnote), so it appears that EA end groups are formed by the transfer of an acyl group to an EG end group.

The randomness of the distribution of repeat units in PET-*co*-OB has been the subject of several studies. Early reports concluded that PET-*co*-OB is a random copolyester,[13,44] but a later study showed that there is a small but measurable deviation from a random distribution of structural units in PET-*co*-OB.[45] Dyad distributions in PET-*co*-OB can be measured by ^{13}C NMR spectroscopy. The chemical shift of the C-4 carbon of the oxybenzoate (B) units are sensitive to the identity of the adjacent structural unit, thereby giving rise to two peaks which determine the ratio of dyad sequences. Previously reported spectra show that these two peaks have additional structure (probably due to triad sequences), but the resolution was not great enough to distinguish the additional peaks.[44]

PET-*co*-OB40, PET-*co*-OA20, and several of the PET-*co*-ON copolymers were studied using ^{13}C NMR spectroscopy to determine the randomness of repeat unit sequences. As shown in Figure 1a, the C-4 carbon of the OB units in PET-*co*-OB40 gives rise to four peaks between 154 and 156 ppm. The two peaks at 155.4 and 155.3 ppm are assigned to B dyads, and the two peaks at 155.0 and 154.8 ppm are assigned to A dyads (Table 2) in accord with previous reports.[46] However, a similar analysis of the region of the spectra corresponding to the oxygen-substituted carbon (C-6) of the ON and OA units of PET-*co*-ON20 and PET-*co*-OA20 indicates the presence of only three peaks in each case, centered at 150.6 and 149.1 ppm, respectively (Figure 1b,c). The overlap of some of the peaks means that dyad information cannot be determined from this region of the spectrum.

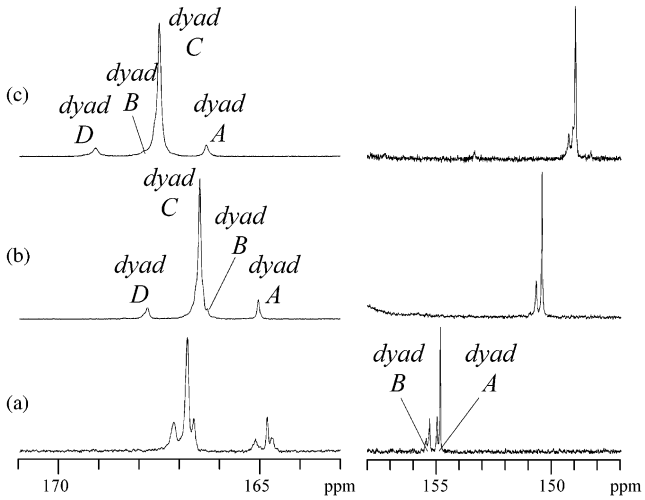

Figure 1. Expanded regions of ^{13}C NMR spectra of (a) PET-*co*-OB40, (b) PET-*co*-ON20, and (c) PET-*co*-OA20 with dyad labels. The peaks with chemical shifts between 164 and 170 ppm are due to carbonyl carbon atoms in both oxyarenecarboxylate units and terephthalate units. The peaks with chemical shifts between 148 and 156 ppm are due to either the C-4 carbon atoms in oxybenzoate units or the C-6 carbon atoms in oxynaphthoate or oxyanthracenoate units.

Table 2. Oxybenzoate-Based Dyads of PET-*co*-OB

		C-4 ^{13}C chemical shift (ppm)
A dyad	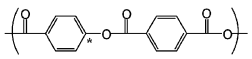	154.9
B dyad	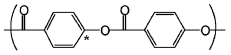	155.35

Considering other carbon atoms for which the chemical shift should be sensitive to repeat unit sequence, we turned our attention to the carbonyl region of the ^{13}C NMR spectra. The carbonyl carbon atoms in PET-*co*-OB40 give rise to multiple peaks (Figure 1a), but they are not resolved well enough to make assignments to repeat unit sequences. However, the carbonyl carbon atoms of the ON and OA oxyarenecarboxylates and the terephthalate (T) structural units in PET-*co*-ON and PET-*co*-OA give rise to well-resolved peaks that can be used to determine the ratio of dyads. For PET-*co*-ON, the chemical shift of the carbonyl carbon atoms on the ON units depends on the neighboring structural units, EG or ON (Table 3). The carbonyl carbon atoms of the terephthalate (T) units also give rise to two peaks based on the adjacent units, EG or N. The peaks for dyads B and C overlap (Figure 1b,c), but the integral values for each can be calculated on the basis of the total ratio of T to ON in the polymer. The PET-*co*-OA copolymers give a similar pattern of peaks in the carbonyl region. The integrals of the peaks arising from dyads A and B can then be used to determine a randomness factor Ψ:[44]

$$\alpha(X_{Ar}) = B/(A + B)$$

$$\alpha°(X_{Ar}) = (X_{Ar})/[X_{Ar} + 2(1 - X_{Ar})]$$

$$\Psi(X_{Ar}) = [\alpha(X_{Ar}) - \alpha°(X_{Ar})]/[1 - \alpha°(X_{Ar})]$$

where $\alpha(X_{Ar})$ is the fraction of oxyarenecarboxylate structural units (Ar = OB, ON, or OA) that are connected directly to another Ar unit in a copolymer

Table 3. Ar-Based Dyads of PET-*co*-ON and PET-*co*-OA

		Carbonyl ^{13}C chemical shift (ppm)	
		PETN	PETA
Ar-based dyads[a]			
A dyad	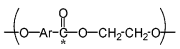	164.9	166.3
B dyad	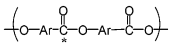	166.2	167.6
T-based dyads			
C dyad	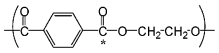	166.4	167.5
D dyad	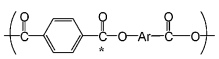	167.7	169.1

[a] Ar = 2,6-naphthalene for PET-*co*-ON and 2,6-anthracene for PET-*co*-OA.

Table 4. Calculated Randomness Factors and Number-Average Sequence Lengths for PET-*co*-OB, PET-*co*-ON, and PET-*co*-OA

	$\Psi(X_{Ar})$	$\Psi(X_T)$	L_{Ar-Ar}	$L°_{Ar-Ar}$	L_{T-T}	$L°_{T-T}$
PET-*co*-OB40	0.06	[a]	1.41	1.33	[a]	[a]
PET-*co*-ON20	0.12	0.10	1.28	1.12	10.0	9.01
PET-*co*-ON30	0.17	0.27	1.46	1.21	7.81	5.68
PET-*co*-ON40	0.32	0.31	1.47	1.33	5.81	4.00
PET-*co*-OA20	0.27	0.26	1.54	1.12	12.2	9.01

[a] Statistics for T-centered dyads in PET-*co*-OB could not be calculated because ^{13}C peaks for the carbonyl carbons were not resolved well enough.

containing X_{Ar} mole fraction of Ar units. $\alpha°(X_{Ar})$ is the fraction of Ar units that would be adjacent to another Ar unit in a totally random copolymer, and $\Psi(X_{Ar})$ is a randomness number for Ar-centered dyads. This randomness factor is zero for purely random copolymer and one for a homopolymer or diblock copolymer. The integrals of the peaks for the dyads C and D can be used in a manner similar to determine $\Psi(X_T)$, a randomness factor based on the T-centered dyads which, like $\Psi(X_{Ar})$, varies from zero to one for random and nonrandom structures. From the calculated randomness factors listed in Table 4 it is evident that PET-*co*-OB, PET-*co*-ON, and PET-*co*-OA are not totally random copolymers, nor are they block copolymers. The number-average sequence lengths of oxyarenecarboxylate and terephthalate segments (L_{Ar-Ar}, and L_{T-T}, respectively) have been calculated[44,47] and are reported in Table 4 along with the theoretical values for random copolymers ($L°_{Ar-Ar}$ and $L°_{T-T}$). The measured sequence lengths are all slightly larger than the theoretical values for a random sequence, which is in agreement with a small deviation from randomness.

The incorporation of oxybenzoate units into PET requires the initial acidolysis transesterification reaction between monomeric acetoxyarenecarboxylic acid and PET, during which the molecular weight of the polymer decreases owing to chain scission and the formation of acetoxyphenyl and terephthalic acid end groups. However, the polymerization (or oligomerization) of the acetoxyarenecarboxylic acid will be a competing process. This proceeds via transfer of the acyl group from the phenolic oxygen to the carboxylic acid to form a reactive acid anhydride and a phenol. The phenol then reacts with the anhydride to form the aryl ester of the type B dyad, with the liberation of acetic acid as the byproduct of the condensation reaction. These dyads will also be formed by transesterification of the acetoxyphenyl end groups formed by acidolysis with acetoxy- or hydroxyarenecarboxylates. It is therefore reasonable that the type B dyads are overrepresented in the polymer. We did not observe changes in randomness upon solid-state polymerizing, as others have noted in certain cases.[46]

Table 5. Thermal Properties of Copolymers

	T_g (°C)	T_m (°C)	ΔH_m (J/g)	T_c (°C)	ΔH_c (J/g)
PET	78	247	35	179	−40
PET-*co*-OB40	80	208	17	159	−12
PET-*co*-ON20	82	210	25	160	−21
PET-*co*-ON30	76	206	19	164	−16
PET-*co*-ON40	79	204	11	157	−7
PET-*co*-OA10	83	234	33	173	−33
PET-*co*-OA15	84	223	26	168	−27
PET-*co*-OA20	87	209	22	156	−18
PET-*co*-OA30	88	206	9	150	−7
PET-*co*-OA40	96	206	3	146	−2

Thermal Analysis. Thermal transitions from DSC analysis of PET-*co*-OB, PET-*co*-ON, and PET-*co*-OA are given in Table 5. The PET-*co*-ON copolymers display a glass transition temperature (T_g) similar to that of PET (78 °C), whereas the PET-*co*-OA copolymers show an increase in T_g as the mol % of OA units increases. This increase in T_g is similar to that reported for PET-*co*-2,6-anthracenedicarboxylate and is attributed to the rigid nonlinear anthracene units that increase chain stiffness and thus increase the temperature needed for the onset of segmental motion.[48]

All of the copolymers in Table 5 are semicrystalline, so their DSC heating curves all have endothermic melting peaks (T_m) and the cooling curves all have exothermic crystallization peaks (T_c). The addition of OB, ON, or OA units to PET disrupts crystalline packing and has the effect of lowering the melting temperature and the crystallization temperature as well as the heat of melting (ΔH_m) and the heat of crystallization (ΔH_c). In general, increasing the amount of comonomer causes a decrease in all four of these values. Interestingly, the T_m is lowered as the amount of comonomer increases (T_m decreases from 234 °C for PET-*co*-OA10 to 206 °C for PET-*co*-OA30, for example), but it does not depend much on the structure of the comonomer (PET-*co*-OB40, PET-*co*-ON40, and PET-*co*-OA40 all melt at 204−208 °C). For the higher composition copolymers, the melting and crystallization peaks are broad and small. The degree of crystallinity decreases as the amount of comonomer increases (ΔH_m = 33 and 9 J/g for PET-*co*-OA10 and PET-*co*-OA30, respectively), and it also decreases as the length of the comonomer increases (ΔH_m = 17, 11, and 3 J/g for PET-*co*-OB40, PET-*co*-ON40, and PET-*co*-OA40, respectively). The values of T_c and ΔH_c follow trends similar to those for the values of T_m and ΔH_m, with T_c dependent on the amount, but not so much on the identity, of the commoner. ΔH_m is dependent on both the amount and the identity of the comonomer.

Despite the diminishment and slowing of crystallization in the copolymers, none of the second heating curves had exothermic peaks for cold crystallization upon subsequent cooling. DSC scans of PET-*co*-OB compositions which are known LCPs do not show a peak for a nematic-to-isotropic transition, and PET-*co*-OB decomposes before it melts into an isotropic phase.[16,49] The DSC heating curves of PET-*co*-ON and PET-*co*-OA copolymers also did not have endothermic peaks at temperatures above T_m (up to 400 °C).

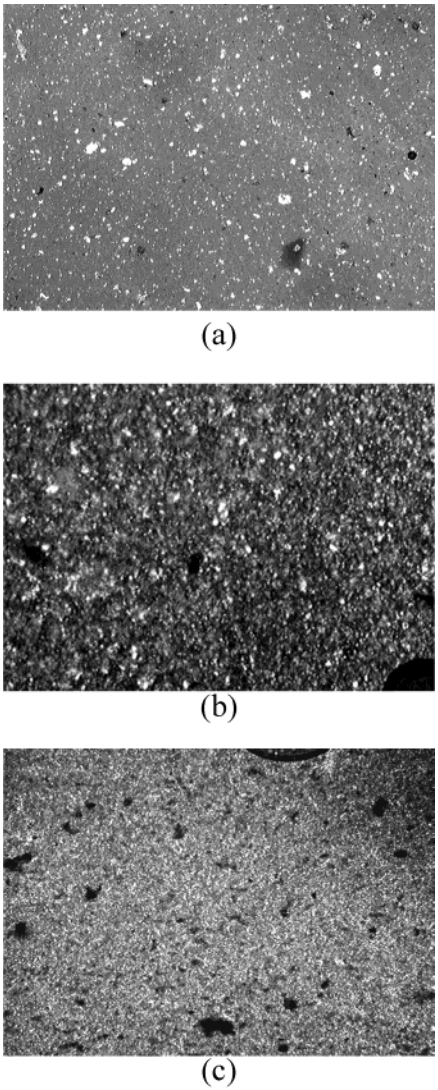

Figure 2. Polarized light photomicrographs of (a) PET-*co*-OA10 at 250 °C, (b) PET-*co*-OA15 at 250 °C, and (c) PET-*co*-OA20 at 250 °C.

Polarized Optical Microscopy. When they are observed under a polarizing microscope, LCPs typically display birefringent textures that are consistent with anisotropic mesophases. Polarized light micrographs of PET-*co*-OB30 are reported to be mostly dark images with a few small bright crystallites when heated above T_m.[16] The bright spots disappear when the temperature is increased to 275 °C. When the amount of OB units is increased to 40 mol % or greater, polarized light micrographs of PET-*co*-OB show bright colorful textures in support of their liquid crystallinity.[16]

As with PET-*co*-OB30, polarized light micrographs of PET-*co*-ON20 and PET-*co*-OA10 show mostly dark images with small bright domains when heated above T_m (Figure 2a). The birefringent domains remain even when the samples are heated to 350 °C. The appearance of these ordered domains can be explained by the presence of aggregates of ON- or OA-rich sequences which orient the surrounding PET chains. Upon increasing the amount of the anthracene monomer to 15 mol %, the polarized optical micrographs of PET-*co*-OA15 appear similar to those of PET-*co*-OA10, except that the crystallites are much larger and account for almost half of the area in the micrograph (Figure 2b).

Further increases in the concentration of the anthracenate monomer results in the formation of a fluid phase above T_m which displays bright birefringence, similar to copolymers containing larger amounts of the benzoate and naphthoate structural units (PET-*co*-OB40 and PET-*co*-ON30) (Figure 2c). The birefringent textures of the PET-*co*-ON and PET-*co*-OA samples appear similar to those previously reported for liquid crystalline compositions of PET-*co*-OB.[16] The bright textures remain even when the samples are heated to 350 °C. Micrographs of samples with >30% ON or >20% OA look similar to those shown in Figure 1c, but the copolymers are more viscous than PET-*co*-OA20 and do not appear to flow unless the samples are sheared. Thus, the amount of OB, ON, or OA units required to make PET-based LCPs varies inversely with the aspect ratio of the oxyarenecarboxylate unit. The rigidity of the backbone required for onset of liquid crystallinity is achieved by adding only 20 mol % of the OA unit, compared to 30% ON or 40% OB.

The mesophases of these LCPs all have a broad range of thermal stability. There is no indication of melting into an isotropic phase below 350 °C by optical microscopy (400 °C by DSC). T_m values are all between 204 and 209 °C. While PET-*co*-OB40 has only linear 1,4-phenylene aromatic subunits, its T_m is similar to those of PET-*co*-ON40 and PET-*co*-OA40, which both have longer aromatic units and might be expected to have higher T_m values. However, noncollinearity of the oxyarenecarboxylate units (ON and OA) in the polymer backbone reduces chain interactions and is at least partially responsible for the low melting temperatures. In contrast to these oxyarenecarboxylate-containing polymers, polymers with symmetrically substituted 2,6-naphthalenedicarboxylate and 2,6-anthracenedicarboxylate units do not form liquid crystalline phases. This further illustrates the need for unsymmetrical units which possess a permanent dipole in the design of mesogenic units for main chain LCPs.

X-ray Analysis. Three of the LC copolymers were examined by wide-angle X-ray scattering. At room temperature, the wide-angle X-ray diffraction (WAXD) trace of PET-*co*-OB40 shows a broad amorphous halo with a crystalline structure superimposed on top of it. These peaks (2θ = 17.0°, 18.5°, and 26.5°) correspond to some of the peaks in the WAXD pattern for crystalline PET. However, because the extent of crystallinity in PET-*co*-OB40 is much lower than that in PET (ΔH_m = 17 and 35 J/g for PET-*co*-OB40 and PET, respectively), the diffraction peaks for the copolymer are small and broad, as shown previously.[16] The WAXD traces for PET-*co*-ON30 and PET-*co*-OA20 at room temperature are similar to that of PET-*co*-OB40. The crystalline peaks disappear from the WAXD traces of all three copolymers when they are heated above T_m, leaving only a broad peak at 2θ = 19°. This lack of a well-defined lattice above T_m is in agreement with reports of WAXD traces for other nematic LC polyesters.[50−52]

Conclusions

Copolymers of PET that contain ≥30 mol % 2,6-oxynaphthoate units (ON) or ≥20 mol % 2,6-oxyanthracenoate units (OA) form similar liquid crystalline phases which are similar to that formed by PET-*co*-OB containing ≥40 mol % of 4-oxybenzoate structural unit (OB). The molar amount of oxyarenecarboxylate units required for liquid crystallinity in these copolymers

decreases as the length of the oxyarenecarboxylate unit increases. The incorporation of the oxyanthracenoate unit into copolymers will allow for further modification of the polymer by Diels−Alder reactions[21,53] and photodimerization.[54]

Acknowledgment. We thank KoSa for support of our program in modified polyesters and Tamas Varga for acquiring WAXD data. J.H. (a visiting undergraduate research student from the University of Indianapolis) and W.R. were supported by the NSF−REU program (NSF-9820252) at GIT.

References and Notes

(1) Weiss, R. A., Ober, C. K., Eds.; *Liquid Crystalline Polymers*; ACS Symposium Series 435; American Chemical Society: Washington, DC, 1990.
(2) Carfagna, C., Ed.; *Liquid Crystalline Polymers*; Pergamon: Oxford, 1994.
(3) Ciferri, A., Ward, I. M., Eds.; *Ultrahigh Modulus Polymers*; Applied Sciencs: London, 1979.
(4) Suenaga, J. *Polym. News* **1990**, *15*, 201.
(5) East, A. J.; Golder, M. Polyesters, Thermoplastic. In *Kirk-Othmer Encyclopedia of Chemical Technology*, 4th ed.; Kroschwitz, J. I., Ed.; Wiley-Interscience: New York, 1996; Vol. 19, pp 641−647.
(6) *Plast. News*, March 6, 2000, p 23.
(7) Morse, P. M. *Chem. Eng. News* **1997**, *75*, 8.
(8) Defosse, M. *Mod. Plast.* **2002**, *79*, 51.
(9) Tonelli, A. E. *Polymer* **2002**, *43*, 637.
(10) Guo, M.; Brittain, W. J. *Macromolecules* **1998**, *31*, 7166.
(11) Welsh, G. E.; Blundell, D. J.; Windle, A. H. *Macromolecules* **1998**, *31*, 7562.
(12) Aoki, Y.; Li, L.; Amari, T.; Nishimura, K.; Arashiro, Y. *Macromolecules* **1999**, *32*, 1923.
(13) Jackson, W. J., Jr.; Kuhfuss, H. F. *J. Polym. Sci., Polym. Chem. Ed.* **1976**, *14*, 2043.
(14) Kuhfuss, H. F.; Jackson, W. J. U.S. Pat. 3 778 410, 1973 (Tennessee Eastman).
(15) Kuhfuss, H. F.; Jackson, W. J. U.S. Pat. 3 804 805, 1974 (Tennessee Eastman).
(16) Kang, T.; Ha, C. *J. Appl. Polym. Sci.* **1999**, *73*, 1707.
(17) Li, X.; Huang, M.; Guan, G.; Sun, T. *J. Appl. Polym. Sci.* **1997**, *66*, 2129.
(18) Liu, Yongjian; Jin, Y.; Dai, L.; Bu, H.; Luise, R. R. *J. Polym. Sci., Polym. Chem. Ed.* **1999**, *37*, 369.
(19) Liu, Y. *Macromol. Chem. Phys.* **2001**, *202*, 488.
(20) Economy, J.; Storm, R. S.; Matkovich, V. I.; Cottis, S. G.; Nowak, B. E. *J. Polym. Sci., Polym. Chem. Ed.* **1976**, *14*, 2207.
(21) Jones, J. R.; Liotta, C. L.; Collard, D. M.; Schiraldi, D. A. *Macromolecules* **1999**, *32*, 5786.
(22) Ma, H.; Hibbs, M.; Collard, D. M.; Kumar, S.; Schiraldi, D. A. *Macromolecules* **2002**, *35*, 5123.
(23) Liu, R. Y. F.; Hu, Y. S.; Hibbs, M. R.; Collard, D. M.; Schiraldi, D. A.; Hiltner, A.; Baer, E. *J. Polym. Sci., Part B: Polym. Phys.* **2003**, *41*, 289. Hu, Y. S.; Liu, R. Y. F.; Rogunova, M.; Schiraldi, D. A.; Nazarenko, S.; Hiltner, A.; Baer, E. *J. Polym. Sci., Part B: Polym. Phys.* **2002**, *40*, 2489. Nowick, J. S.; Feng, Q.; Tjivikua, T.; Ballester, P.; Rebek, J., Jr. *J. Am. Chem. Soc.* **1991**, *113*, 8831.
(24) Taber, D. F.; Sethuraman, M. R. *J. Org. Chem.* **2000**, *65*, 254.
(25) Thiele, J.; Giese, O. *Chem. Ber.* **1903**, *36*, 843.
(26) Ihmels, H. *Eur. J. Org. Chem.* **1999**, *7*, 1598.
(27) Kelly, T. R.; Parekh, N. D.; Trachtenberg, E. N. *J. Org. Chem.* **1982**, *47*, 5009.
(28) Morgan, G.; Coulson, E. *J. Chem. Soc.* **1929**, 2203.
(29) Skorokhodov, S. S.; Rudaya, L. I.; Klimova, N. V.; Bol'shakov, M. N. *Russ. J.*
(30) *Appl. Chem.* **1998**, *71*, 2164.
(31) Dougherty, G.; Gleason, A. H. *J. Am. Chem. Soc.* **1930**, *52*, 1024.
(32) Gundermann, K. D.; Klockenbring, G.; Roker, C.; Brinkmeyer, H. *Justus Liebigs Ann. Chem.* **1976**, 1873.
(33) Hayashi, M. J. *J. Chem. Soc.* **1927**, 2516. (b) Danielsen, K. *Acta Chem. Scand.* **1996**, *50*, 954.
(34) Singh, A.; Andrews, L. J.; Keefer, R. M. *J. Am. Chem. Soc.* **1962**, *84*, 1179.
(35) Bradlow, H. L.; VanderWerf, C. A. *J. Am. Chem. Soc.* **1947**, *69*, 1254.
(36) Baltzly, R.; Buck, J. S. *J. Am. Chem. Soc.* **1943**, *65*, 1984.
(37) West, C. T.; Donnelly, S. J.; Kooistra, D. A.; Doyle, M. P. *J. Org. Chem.* **1973**, *38*, 2675.
(38) Mills, S. G.; Beak, P. *J. Org. Chem.* **1985**, *50*, 1216.
(39) Criswell, T. R.; Klanderman, B. H. *J. Org. Chem.* **1974**, *39*, 770.
(40) Kuzuya, M.; Miyake, F.; Kamiya, K.; Okuda, T. *Tetrahedron Lett.* **1982**, *23*, 2593.
(41) Doering, W. v. E.; Kitagawa, T. *J. Am. Chem. Soc.* **1991**, *113*, 4288.
(42) Fieser, L. F.; Lothrop, W. C. *J. Am. Chem. Soc.* **1936**, *58*, 749.
(43) Han, X.; Williams, P. A.; Padias, A. B.; Hall, H. K., Jr.; Linstid, H. C.; Sung, H. N.; Lee, C. *Macromolecules* **1996**, *29*, 8313.
(44) McFarlane, F. E.; Nicely, V. A.; Davis, T. G. *Contemporary Topics in Polymer Science*; Pierce, E. M., Schaefgen, J. R., Eds.; Plenum: New York, 1977; Vol. 2, p 109.
(45) Nicely, V. A.; Dougherty, J. T.; Renfro, L. W. *Macromolecules* **1987**, *20*, 573.
(46) Lenz, R. W.; Jin, J.; Feightinger, K. A. *Polymer* **1983**, *24*, 327.
(47) Ibbett, R. N. *NMR Spectroscopy of Polymers*; Blackie Academic & Professional: London, 1993; p 50.
(48) Kriegel, R. M.; Collard, D. M.; Liotta, C. L.; Schiraldi, D. A. *Macromol. Chem. Phys.* **2001**, *202*, 1776.
(49) Meesiri, W. *J. Polym. Sci., Polym. Phys. Ed.* **1982**, *20*, 719.
(50) Romo-Uribe, A.; Windle, A. H. *Macromolecules* **1996**, *29*, 6246.
(51) Acierno, D.; Amendola, E.; Concilio, S.; Fresa, R.; Iannelli, P.; Vacca, P. *Macromolecules* **2000**, *33*, 9376.
(52) Flores, A.; Ania, F.; Balta Calleja, F. J.; Ward, I. M. *Polymer* **1993**, *34*, 2915.
(53) Vargas, M.; Kriegel, R. M.; Collard, D. M.; Schiraldi, D. A. *J. Polym. Sci.* **2002**, *40*, 3256.
(54) Jones, J. R.; Liotta, C. L.; Collard, D. M.; Schiraldi, D. A *Macromolecules* **2000**, *33*, 1640.

MA034425S